PHYSICAL REVIEW B VOLUME 28, NUMBER 8 15 OCTOBER 1983

Nonradiative transitions by path integrals with the use of semiclassical approximations

A. Agresti
Istituto di Ricerca sulle Onde Elettromagnetiche del Consiglio Nazionale delle Ricerche, I-50127 Firenze, Italy and Dipartimento di Fisica dell'Università degli Studi di Firenze, I-50127 Firenze, Italy

D. Mugnai
Istituto di Ricerca sulle Onde Elettromagnetiche del Consiglio Nazionale dell Ricerche, I-50127 Firenze, Italy and Scuola di Perfezionamento in Fisica dell'Università degli Studi di Firenze, I-50127 Firenze, Italy

A. Ranfagni
Istituto di Ricerca sulle Onde Elettromagnetiche del Consiglio Nazionale delle Ricerche, I-50127 Firenze, Italy

R. Englman
Soreq Nuclear Research Center, Yavne 70600, Israel
(Received 29 September 1982)

Tunneling transition rates are evaluated for a two-mode system in the semiclassical (WKB) approximation with inclusion of contributions of neighboring paths to the classical one, connecting two given points, or by considering a distribution of classical paths. Neighboring paths increase the transmission coefficient in the cases of single—saddle-point barrier by about 6%, while in the cases of two or three saddle points this rise can reach 100%. Thus the consideration of several classical paths is important if there are several least-action paths, e.g., for symmetry reasons. This formalism is then applied to nonradiative transitions occurring in color centers. In particular, we reconsider the temperature dependence of the A_T and A_X emissions in Tl^+ centers, which is a typical case of three—saddle-point barrier.

I. INTRODUCTION

The usefulness of the semiclassical (WKB) approximation has been recently emphasized in various fields of physics such as collision theory and molecular and solid-state physics.[1–10] Particular attention has been paid to nonradiative processes occurring in systems with complex potential surfaces in multidimensional spaces.[3,6,9,11]

Here the basic problem is the evaluation of the probability for a system in going from a given point to another in a suitable space-time manifold. According to the Feynman path-integral method,[12–14] the problem can be attacked by considering the contribution over all the paths connecting the two given points. Such a procedure, however, encounters severe limitations, mainly because of normalization problems. It becomes amenable when the Lagrangian of the systems is a quadratic form of the coordinates and velocities, since in this case the amplitude of probability depends on the action integral S_{cl} taken only along the classical path. When the potential is a slowly varying function of the coordinates, or for quasiclassical systems, the amplitude can still be approximately expressed by S_{cl} (WKB approximation), even in multidimensional nonseparable problems, by assuming that the system moves only along the classical trajectory.[11]

A criterion for judging the validity of this procedure was given in Ref. 15 on the basis of the geometrical characteristics of the trajectory. Such a criterion, however, is not easily applicable in practical cases. This problem has recently been reconsidered by including in the analysis of the tunneling transition the contribution of all the neighboring paths to the classical path and suggesting a simple normalization rule.[16] On this basis, we consider in this paper the problem of the nonradiative transition between minima situated on multidimensional potential surfaces. In Secs. II and III a new method of evaluating the transmission coefficient, with inclusion of neighboring paths to the classical path, is derived. This procedure on one hand justifies the usual approximation of considering only one contribution, that corresponding to the classical trajectory; on the other hand, it allows us to extend the evaluation to the cases of nearly coincident classical trajectories, as well as the continuous distributions of classical paths. This analysis will then be applied to study the emission intensity behavior of luminescent centers in ionic crystals. In Sec. IV we examine the temperature dependence of the emission intensity as originating by optical transition from a double-well excited-state potential model. Here, rather general expressions are derived, including tunneling and back-tunneling from one minimum to the other. Then we apply the results of Secs. II and III to the case of a Tl^+ impurity in alkali halides, obtaining a sensible improvement of the capability of the model in explaining the experimental data with respect to the method used in a previous work.[6] The approximations involved are then discussed in Sec. V.

II. TRANSMISSION COEFFICIENT IN MULTIDIMENSIONAL PROBLEMS

Let us consider the transmission across a barrier in a multidimensional space between an initial point (i) in the left-hand well and a representative final point (f) in the

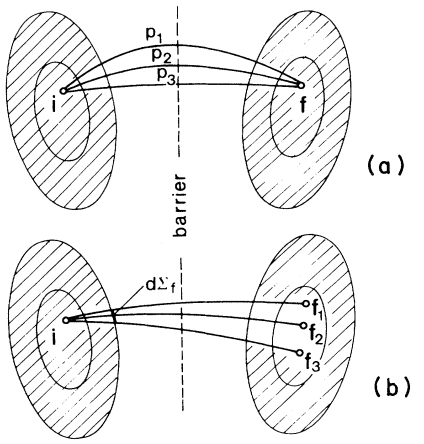

FIG. 1. Transmission across a potential barrier between two potential minima (shading represents classically allowed regions, where $E > V$). (a) Several pathways, leading from the initial point (i) to a representative final point (f), one of which is the least-action path or classical path; (b) A set of classical paths, leading to a set of ending points in the neighborhood of f, passing across a section $d\Sigma_f$ of the initial well.

right-hand well. The situation in a two-dimensional space is shown in Fig. 1(a). There are several pathways $p_1, p_2, \ldots$ leading to f. The wave function based on path integrals is a sum of the contributions

$$\psi(i \to f) = \sum_{p = p_1, p_2, \ldots} \psi_p(i \to f) \ .$$

In the classical allowed region ($E > V$), shown by shading, the partial waves ψ_p strongly fluctuate and tend to cancel one another, except for p near the classical path (where the action integral is stationary[12]) and therefore, approximately

$$\psi_p(i \to f) = A e^{iS_{\rm cl}(i,f)/\hbar} \ . \tag{1}$$

The density of current is given by[17]

$$\vec{j} = \frac{\hbar}{2i\mu}(\psi^* \vec{\nabla}\psi - \psi \vec{\nabla}\psi^*) \ .$$

By substituting ψ as given by Eq. (1), we have

$$\vec{j}(i \to f) = \frac{1}{\mu} A^2 \vec{\nabla} S(i,f) = \frac{1}{\mu} |\psi_p(i \to f)|^2 \vec{\nabla} S(i,f) \ . \tag{2}$$

The classical path $i \to f$ for sub-barrier energies will transpierce the left-hand potential well at some point. The set of classical paths leading to a set of points in the neighborhood of f will pass across a section $d\Sigma_f$ of the initial well [for a two-dimensional system $d\Sigma_f$ will be a curved line element; see Fig. 1(b)]. Neighboring contributions to the current element $d\mathcal{J}$ will be

$$d\mathcal{J} = j(i \to f) d\Sigma_f \ .$$

Integrating over the set of point f in the right well, we have the current

$$\mathcal{J}(i \to \text{right}) = \int_{\Sigma_{\rm in}} j(i \to f) d\Sigma_f \ , \tag{3}$$

where $\Sigma_{\rm in}$ is the total section of the left-hand well across which particles travel from i to the right-hand well by classical motion. (Particles going across the left-hand well outside $\Sigma_{\rm in}$ do not get to the right-hand well.)

The WKB wave function, along a classical path (p) connecting the initial point (i) and a generic final point (f) in the right-hand well, is expressed as[15]

$$\psi_p(s) = B(|\vec{\nabla} S| \Sigma)^{-1/2} e^{iS_{\rm cl}(i,f)/\hbar} \ , \tag{4}$$

where B is a constant, Σ is the normal section of the flux tube. In the barrier region the wave function [Eq. (4)] will be attenuated according to the factor $e^{-|S|/\hbar}$, S being the action integral between the two classical turning points a and b [$V(a) = V(b) = E$].

By substituting Eq. (4) into Eqs. (2) and (3) and identifying Σ with $\Sigma_{\rm in}$, we see, after integration, that the incident current is simply given by

$$\mathcal{J}_{\rm in} = B^2/\mu$$

(this is true if B^2 can be considered as independent of Σ; if this is not the case, B^2 must be replaced by a suitable mean value).

Analogously, the current outgoing from the barrier region is expressed as

$$\mathcal{J}_{\rm out} = \frac{1}{\mu} \frac{B^2}{\Sigma_{\rm out}} \int_{\Sigma_{\rm out}} e^{-2S_{a,b}(\Sigma)/\hbar} d\Sigma \ ,$$

where $S_{a,b}(\Sigma)$ is a function of Σ since it depends on the path. The transmission coefficient is the ratio of the transmitted and incident currents and turns out to be

$$D \equiv \frac{\mathcal{J}_{\rm out}}{\mathcal{J}_{\rm in}} = \frac{1}{\Sigma_{\rm out}} \int_{\Sigma_{\rm out}} e^{-2S_{a,b}(\Sigma)/\hbar} d\Sigma \ . \tag{5}$$

In order to evaluate the transmission coefficient with Eq. (5) in practical cases, one must define $\Sigma_{\rm out}$. A critical analysis of this point has been given elsewhere.[16] Here we limit ourselves to the following considerations. First, we wish to note that Eq. (5) contains as a limiting case the usual approximation of considering only one contribution, that corresponding to only one path. This is the case when the flux tube is very narrow ($\Sigma_{\rm out} \to 0$), so that $\Sigma_{\rm out}^{-1}$ in Eq. (5) behaves as a δ function, and we have

$$\lim_{\Sigma_{\rm out} \to 0} \int_{\Sigma_{\rm out}} e^{-2S_{a,b}(\Sigma)/\hbar} \frac{d\Sigma}{\Sigma_{\rm out}} = e^{-2S_0(a,b)/\hbar} \ .$$

The same result is obtained, for any finite value of $\Sigma_{\rm out}$ when $S_{a,b}$ is independent of Σ (multidimensional separable problems).

More generally, it is convenient to consider an expansion of S in powers of Σ ($\ddot{S} = d^2S/d\Sigma^2$),

$$S(\Sigma) = S_0 + \ddot{S}_0 \frac{\Sigma^2}{2} + \cdots \ ,$$

where the linear term is missing since the path for $\Sigma = 0$ is assumed to have the minimum value of S ($= S_0$). If it is

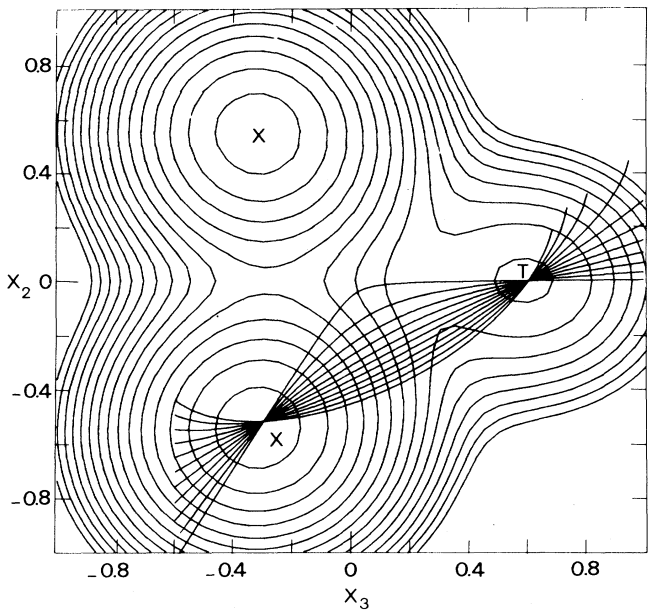

FIG. 2. Potential map of the ${}^3T_{1u,z}$ state in the subspace of the tetragonal Q_2,Q_3 distortions with a family of curves [Eq. (8)] connecting the tetragonal T minimum and one of the two rhombic X minima. Parameter values: $A=3$, $g=0.4$, $\phi\equiv\tan^{-1}m=0,0.1,0.2,\ldots,1$. Each contour line corresponds to an increment of 0.1ζ in the range -1.4ζ–0.

admissible to stop at the quadratic term in Σ, Eq. (5) can be integrated to give

$$D\simeq\left[\frac{\pi\hbar}{\ddot{S}_0}\right]^{1/2}\frac{e^{-2S_0(a,b)/\hbar}}{\Sigma_{\text{out}}}\ . \tag{6}$$

Taking $\Sigma_{\text{out}}=2(\hbar\ln 2/\ddot{S}_0)^{1/2}$, which corresponds to the width at half-height of the function $e^{-2S(\Sigma)}$, we simply obtain[16]

$$D\simeq 1.06e^{-2S_0(a,b)/\hbar}\ . \tag{7}$$

This expression becomes exact in the case where the action is a pure quadratic expression of Σ. Therefore, also in this case the transmission coefficient is nearly coincident with the contribution of one path alone, that corresponding to the easiest path connecting the two minima through the saddle point of the barrier. Equation (6) can be modified for the cases of two or three saddle points closely placed in the Σ space. In the next section we shall see how this problem is worked out in the case of three saddle points.

III. TRANSMISSION COEFFICIENT ON THE ${}^3T_{1u}$ POTENTIAL SURFACES: $T\otimes(\epsilon+\lambda)$, JAHN-TELLER PROBLEM

In this section we shall apply the results of Sec. II to a concrete case, namely to the evaluation of the transmission coefficient in going from a tetragonal minimum (T) to the two lower-lying rhombic minima (X) situated on the potential surface ${}^3T_{1u}$ in the two-dimensional space of tetragonal (Q_2,Q_3) coordinates. The relevance of this potential model has been demonstrated especially in connection with excited-state impurity centers as Tl^+ in alkali halides and other luminescent systems.[18] Here we shall reconsider the problem of the double-emission band (A_T and A_X) of Tl^+ impurity under excitation in the A band.[6] Accordingly, we must evaluate the nonradiative transition rate, as function of the temperature, in going from the T minimum (from which the high-energy emission A_T originates, after optical excitation) to the X minima (from which the low-energy emission A_X arises). Figure 2 shows a potential map of the ${}^3T_{1u,z}$ state, obtained by diagonalizing the Jahn-Teller and spin-orbit Hamiltonian, for the $a_{1g}t_{1u}$ electron configuration in O_h symmetry.[18] The shape of the potential suggests that we look for one or more classical trajectories connecting T and X minima, through the intermediate saddle point, in the form of conical curves. Defining normalized ionic displacements coordinates through $x_{2,3}=-[b/(2\sqrt{3}\zeta)]Q_{2,3}$, the curves are given by

$$x_2=\frac{1}{m+2/\sqrt{3}}(x_3-\{x_3^2[1-m(m+2/\sqrt{3})]+(B/A)^2m(m+2/\sqrt{3})\}^{1/2})\ , \tag{8}$$

where m is the angular coefficient of the straight line tangent to the curve at the upper minimum T, whose coordinates are $x_2=0$, $x_3=B/A$ $(B\sim 2)$. The tangent is in fact given by

$$x_2=m(x_3-B/A)\ . \tag{9}$$

The quantity $A=12(1-\beta)\zeta/b^2$ is a dimensionless parameter, which, together with $g=G/\zeta$, determines the shape of the potential map.[18] For $m<1/\sqrt{3}$ Eq. (8) represents an hyperbola, for $m=1/\sqrt{3}$ a straight line, and for $m>1/\sqrt{3}$ an ellipse. A family of these curves is drawn in Fig. 2.

We have computed the action integral for several paths characterized by a set of parameters m and for different values of the energy E inside the upper minimum T. In terms of the variables and parameter here adopted, the action integral is given by[6]

$$\frac{S}{\hbar}=\frac{2A^{1/2}\zeta}{\hbar\omega}\int_a^b\left[\frac{V-E}{\zeta}\right]^{1/2}ds\ , \tag{10}$$

where a and b denote the turning points ($V=E$) on the selected path. Figure 3 (solid lines) shows some numerical results as a function of the angle $\phi=\tanh^{-1}m$ (negative values of ϕ correspond to paths connecting the initial minimum T with the other minimum X). The least-action paths, for each energy value E, are identified with the minima of the curves $S(\phi)$.

In order to evaluate the "total" nonradiative transition rate in going from the initial minimum (T) to the final ones (X), we must consider all classical paths starting from the initial minimum and ending in the valley region of X minima. This would require repeating the above procedure for each point situated in the X region (and not just

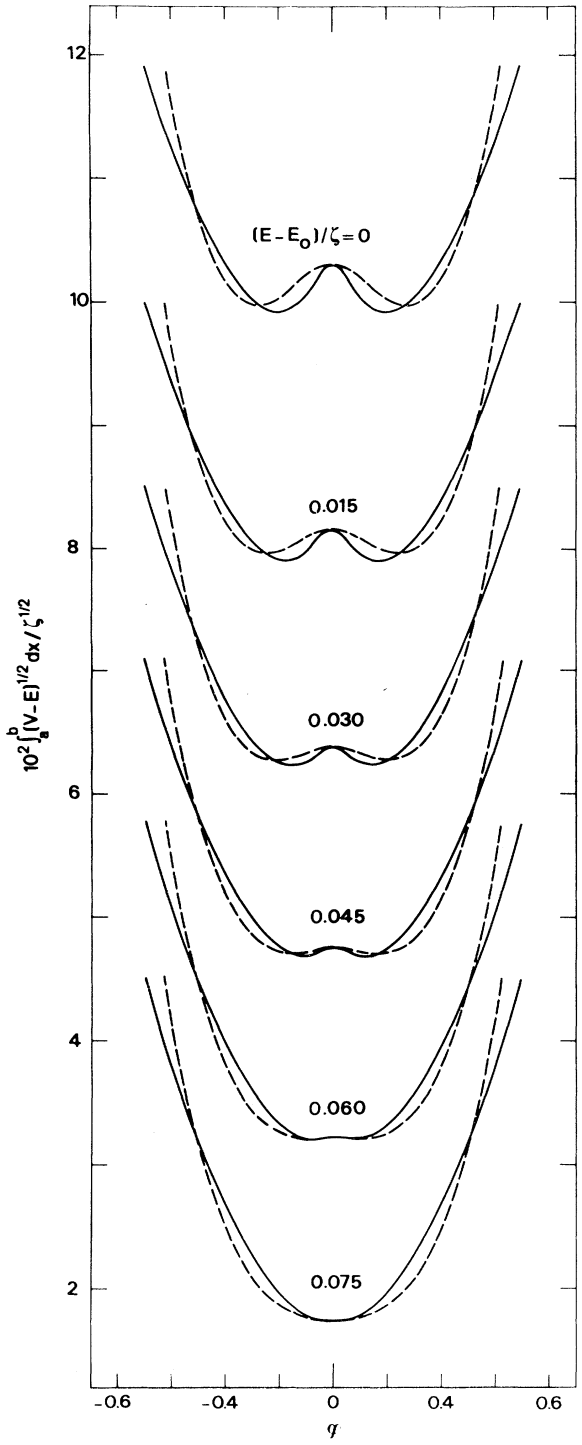

FIG. 3. Action integral (S) as a function of the angle $\phi=\tan^{-1}m$ for different values of the energy inside the upper minimum T. Solid lines represent numerical results obtained along the curves of Fig. 2 [Eq. (8)]. For a given energy, the classical paths connecting T with the two X minima are identified with the minima of the curve $S(\phi)$. These minima tend to coalesce with increasing energy. Dashed curves represent numerical results relative to the tangents [Eq. (9)], going from the initial minimum T, which approximate the classical paths ending in the X-minima region.

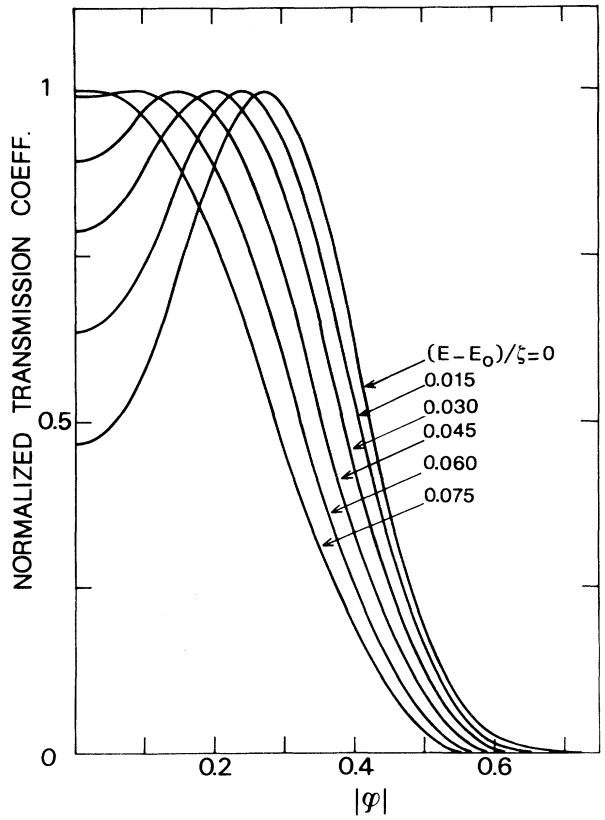

FIG. 4. Transmission coefficient $\exp\{-2\hbar^{-1}[S(\phi)-S_{\min}]\}$, normalized to its maximum value corresponding to the minima of Fig. 3, as a function of the angular variable ϕ and for different values of the energy inside the initial T minimum.

the X point). However, considering the shape of the barrier region [which alone enters in the evaluation of the transmission coefficient, see Eq. (10)] we have approximately solved this problem by replacing the initial portion of the classical paths with the tangent outgoing from the initial minimum T, as given by Eq. (9). The action integrals, as evaluated along these paths, are also reported in Fig. 3 by dashed lines, showing in the minimum regions of the action integral a behavior similar to the solid lines. Therefore, at least in this case, the problem of including contributions from several classical paths is nearly coincident with that of including contributions from the neighboring (nonclassical) paths to a given classical trajectory. Figure 4 shows the normalized transmission coefficient as a function of the angular variable ϕ for different values of the normalized energy $(E-E_0)/\zeta$ inside the initial well (E_0 is the value of the energy in the upper minimum T; ζ is the spin-orbit coupling constant). For lower-lying levels, this function presents two distinct maxima [one for positive (ϕ_1) and the other for negative ($-\phi_1$) values of ϕ], while, with increasing energy, these two maxima tend to coalesce tending to a bell-shaped function. The total transmission coefficient has been evaluated by Eq. (5), where $\Sigma=\rho\phi$, so that

$d\Sigma/\Sigma_{\text{out}}=d\phi/\bar{\phi}$, and the integral has been evaluated by the saddle-point approximation. For the cases of a single maximum this can be done by Eq. (7), while in the cases of double maxima by a three-saddle point approximation.[19] This is now presented.

The function $S_{a,b}(\Sigma)$ in Eq. (5) can be written as $2\lambda f(\phi)$; this, in turn, can be expressed as a polynomial of a new variable z that describes in the simplest fashion the relevant saddle-point arrangement at $\phi=0$. In such a way we have

$$-2\frac{S_{a,b}(\Sigma)}{\hbar}\equiv 2\lambda f(\phi)=a_0-(a+z^2)^2 ,$$

where $\lambda=2A^{1/2}\zeta/\hbar\omega$, $a_0=f(0)<0$, and $a=[f(\phi_1)-f(\phi=0)]^{1/2}$. After substitution into Eq. (5) we get[19]

$$D=(\bar{\phi})^{-1}\left[\frac{4a\pi}{2\lambda^{1/2}\ddot{f}(0)}\right]^{1/2} e^{2\lambda(a_0-a^2/2)}\mathscr{D}_{-1/2}(2\lambda^{1/2}a) , \tag{11}$$

where $\ddot{f}(0)=(d^2f/d\phi^2)_{\phi=0}$ and $\mathscr{D}_{-1/2}(2\lambda^{1/2}a)$ is the parabolic cylinder function[20]

$$\mathscr{D}_{-1/2}(t)=\frac{2e^{t^2/4}}{\sqrt{\pi}}\int_0^\infty e^{-(t+p^2)^2/2}dp .$$

When the two maxima of the function $f(\phi)$ tend to coalesce ($\phi_1\to 0$), Eq. (11) becomes[19]

$$D=(\bar{\phi})^{-1}\frac{\Gamma(\frac{1}{4})}{2(2\lambda)^{1/4}}\left[\frac{24}{f^{(4)}(0)}\right]^{1/4} e^{2\lambda f(0)} , \tag{12}$$

where

$$f^{(4)}(0)=\left[\frac{d^4f}{d\phi^4}\right]_{\phi=0} .$$

As for the parameter $\bar{\phi}$ in Eqs. (11) and (12), this has been chosen, according to the results of Sec. II, as the width at half-height of the Gaussian function fitting the function $\exp[2\lambda f(\phi)]$ (see Fig. 4) in the region of the maximum. This is easily done when the maxima are well separated, or in the opposite limit of coalescence minima, while it is a little more uncertain in the intermediate case.

Following this procedure, we get the important result that when the maxima in Fig. 4 are well pronounced, the total transmission coefficient [as given by Eq. (11)] is nearly equal to twice the value ($D_{\max}$) corresponding to the path of minimum action. The factor of 2 is due to the existence of two X minima and two well-separated classical trajectories for reaching each of them. When these trajectories are closer (with increasing energy inside the initial well T) this factor of 2 decreases and tends to unity when the two maxima of Fig. 4 coalesce into only one maximum at $\phi=0$. In Fig. 5 we report the computed values of $D/D_{\max}$ as a function of the normalized energy inside the initial well.

IV. APPLICATION OF Tl^+ LUMINESCENCE

The theory of Secs. II and III will now be applied to analyze the temperature dependence of the emission intensity of KI:Tl and KBr:Tl. In order to derive the intensities of the two emission bands (A_T and A_X), we must calculate the populations of the wells (T and X) which are governed by the kinetic equations[6]

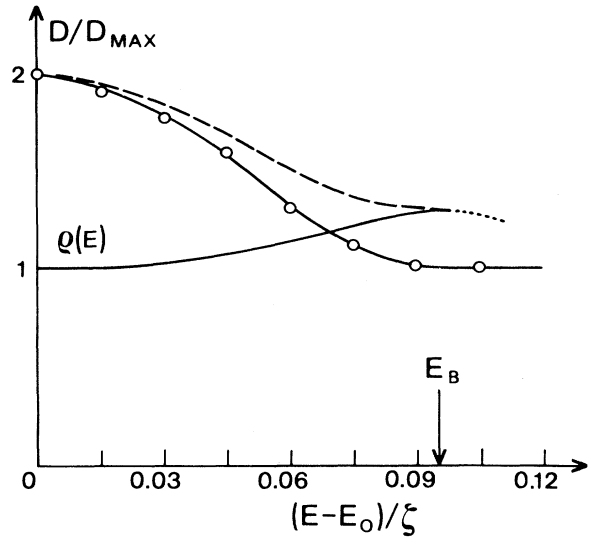

FIG. 5. Total transmission coefficient [Eqs. (11) and (12)], divided by the value corresponding to the path of minimum action, as a function of the normalized energy inside the initial well. The level density $\rho(E)$ is estimated to vary between 1 at the bottom of the well to ~ 1.3 at the top of the barrier (E_b). The dashed line indicates the product $\rho(E)D/D_{\max}$.

$$\begin{aligned}\frac{dC_T}{dt}&=-(W_{T\to X}+\tau^{-1})C_T+W_{X\to T}C_X ,\\ \frac{dC_X}{dt}&=-(W_{X\to T}+\tau^{-1})C_X+W_{T\to X}C_T ,\end{aligned} \tag{13}$$

where $W_{T\to X}$ and $W_{X\to T}$ are the nonradiative transition rates in going from T to X minimum and vice versa and τ^{-1} is the radiative transition rate from the excited to the ground state. By solving the system of differential equations (13) with respect to C_T (or C_X) and integrating, we get

$$\begin{aligned}C(t)=&\,C_1\exp[-(W_{T\to X}+W_{X\to T}+\tau^{-1})t]\\&+C_2\exp(-\tau^{-1}t) .\end{aligned} \tag{14}$$

The intensity is obtained by integrating over t:

$$I=\tau^{-1}\int_0^\infty C(t)dt=\frac{C_1+C_2+(W_{T\to X}+W_{X\to T})\tau C_2}{1+(W_{T\to X}+W_{X\to T})\tau} . \tag{15}$$

The constants C_1 and C_2 obey the following conditions: $C_1^{(T)}+C_2^{(T)}=C_T(t=0)=1$ for the A_T emission (the system is supposed to be prepared initially in the upper T well) and $C_1^{(X)}+C_2^{(X)}=C_X(t=0)=0$ for the A_X emission. The other condition is that the sum $I_{A_T}+I_{A_X}=1$. From these conditions we get

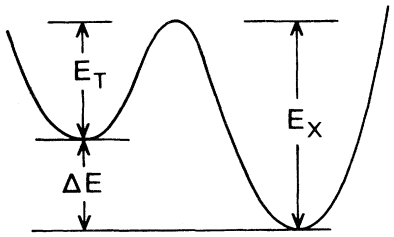

FIG. 6. Double-minimum potential function along the reaction path.

$$I_{A_T}=\frac{1+(W_{T\to X}+W_{X\to T})\tau C_2^{(T)}}{1+(W_{T\to X}+W_{X\to T})\tau}\ ,$$
$$I_{A_X}=\frac{(W_{T\to X}+W_{X\to T})\tau C_2^{(X)}}{1+(W_{T\to X}+W_{X\to T})\tau}\ , \tag{16}$$

where $C_2^{(T)}+C_2^{(X)}=1$.

The intensities, as given by Eqs. (16), are temperature dependent since the $W_{T\rightleftarrows X}$ are functions of the temperature. We further assume that the initial distributions in T and X are thermal. With this assumption,

$$C_2^{(T)}=Ke^{-\Delta E/kT}(1+Ke^{-\Delta E/kT})^{-1}\ ,$$
$$C_2^{(X)}=(1+Ke^{-\Delta E/kT})^{-1}\ , \tag{17}$$

so that the condition $C_2^{(T)}+C_2^{(X)}=1$ is always satisfied. The quantity ΔE corresponds to the energy difference between T and X minima; see Fig. 6. Clearly, when ΔE is sufficiently high, we have $C_2^{(T)}\sim 0$ and $C_2^{(X)}\sim 1$. In this case we can also neglect the back-tunneling ($W_{X\to T}\sim 0$), and Eqs. (16) reduce to

$$I_{A_T}(T)=[1+W_{T\to X}(T)]^{-1}\ ,$$
$$I_{A_X}(T)=1-I_{A_T}(T)\ . \tag{18}$$

These equations are nearly coincident with Eqs. (6) of Ref. 6, apart from the absence of a factor 2 (multiplying $W_{T\to X}$), which is now replaced by an energy-dependent factor entering the expression of $W_{T\to X}$ through the transmission coefficient, which is evaluated according to the results of the preceding section.

To obtain the transition rate $W_{T\to X}$ we can extend the treatment given in Ref. 6 by integrating over all processes that start in the initial well and over all momenta:

$$\frac{W_{T\to X}(T)}{\nu}=\frac{\int d\vec{q}\int d\vec{p}\,\rho(\vec{p},\vec{q})D(\vec{p},\vec{q})e^{-E(\vec{p},\vec{q})/kT}}{\int d\vec{q}\int d\vec{p}\,\rho(\vec{p},\vec{q})e^{-E(\vec{p},\vec{q})/kT}}\ .$$

Here ν is the vibrational frequency within the initial well, $\vec{q}$ is the coordinate vector in the space of the configuration coordinates, $\vec{p}$ is the conjugate momentum, ρ is the density of states in the phase space $\vec{p},\vec{q}$, E is the energy, and D is the transmission coefficient for tunneling that starts at a given point $\vec{q}$ with momentum $\vec{p}$. The expression holds for potential surfaces of any kind.

We shall simplify the above expression in several ways. First, we shall suppose that only processes starting near the optimal path ($\phi=0$ in the preceding section) dominate. Thus the $\vec{q}$ integrals above become one-dimensional. Next, we shall assume that along the path the potential may be considered parabolic; in other words we suppose that tunneling takes place before the anharmonicities in the potential become felt. Last, we only include tunneling processes that start at the (classical) turning points, i.e., with zero initial momentum. The transmission coefficient written as function of the initial energy and position then becomes

$$D(E;q)=D(V(q);q)\ ,$$

and the total transition rate takes the classical form appropriate to a uniform distribution of states in configuration space ($\rho\equiv 1$):

$$\frac{W_{T\to X}(T)}{\nu}=\frac{\int dq\,D(V(q);q)e^{-V(q)/kT}}{\int dq\,e^{-V(q)/kT}}\ .$$

The quantum-mechanical expression arises in this formalism by using a nonuniform distribution of states, $\rho\propto q$. Then

$$\frac{W_{T\to X}(T)}{\nu}=\frac{\int dV\,D(V;q)e^{-V/kT}}{\int dV\,e^{-V/kT}}\ ,$$

and splitting up the range of integration into discrete intervals spaced $\hbar\omega$ apart, one obtains finally

$$\frac{W_{T\to X}(T)}{\nu}=(1-e^{-\hbar\omega/kT})\sum_{n=0}^{\infty}D_n e^{-n\hbar\omega/kT}\ . \tag{19}$$

The transmission coefficient D_n is for the nth quantal level and is evaluated according to Eqs. (11) and (12).

The results for the case of KI:Tl are reported in Fig. 7,

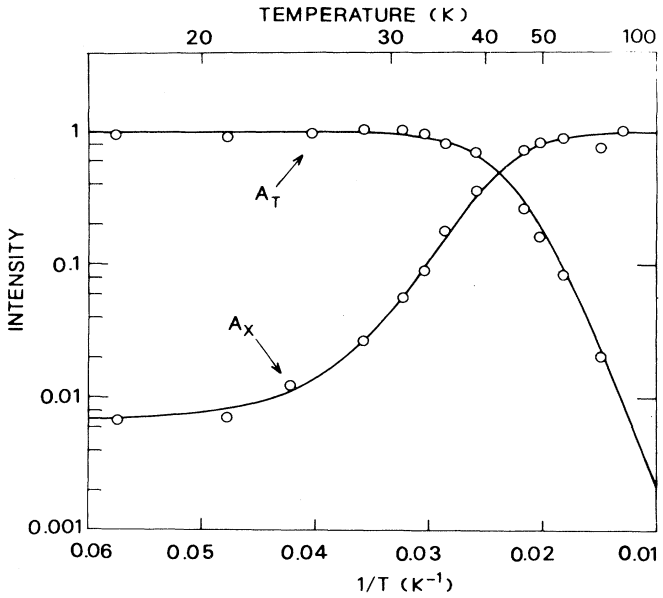

FIG. 7. Temperature dependence of the intensities of the A_T and A_X emission in KI:Tl. ○: experimental data taken from Ref. 21. Solid lines: after Eqs. (18) with $A=3$, $g=0.4$, $\zeta=4114$ cm^{-1}, $\hbar\omega=3.2\times 10^{-2}\zeta$, and $\tau\nu=10^5$.

where by reasonable values of the parameters[6] we get a good agreement with the experimental results.[21] In the case of KBr:Tl, where the temperature behavior of the intensity is more complex, we would have to consider the complete expressions [Eqs. (16)]. However, due to the intrinsic complexity of computing also $W_{X\to T}$ (back-tunneling) by the procedure of Sec. III, we have simply considered approximate expressions of W as (see Fig. 6)

$$W_{T\to X}(T)\sim \nu e^{-E_T/kT}, \qquad W_{X\to T}(T)\sim \nu e^{-E_X/kT}, \tag{20}$$

which correspond to taking into account only the classical contributions and neglecting the quantum tunneling.[11] By substituting Eqs. (17) and (20) into Eqs. (16) we get

$$I_{A_T}(T)=\frac{1+(e^{-E_T/kT}+e^{-E_X/kT})\tau\nu K e^{-\Delta E/kT}(1+Ke^{-\Delta E/kT})^{-1}}{1+(e^{-E_T/kT}+e^{-E_X/kT})\tau\nu},$$
$$I_{A_X}(T)=\frac{(e^{-E_T/kT}+e^{-E_X/kT})\tau\nu(1+Ke^{-\Delta E/kT})^{-1}}{1+(e^{-E_T/kT}+e^{-E_X/kT})\tau\nu}. \tag{21}$$

Figure 8 shows the results obtained together with a best fit of the experimental points by Eqs. (21). The constants (especially E_T, E_X, and ΔE) appear as very reasonable[6,18] even if the low-temperature behavior cannot be well reproduced without considering quantum tunneling.

V. CONCLUDING DISCUSSION

We have shown how to include contributions of neighboring paths to a classical path, connecting two given points corresponding to different potential minima, in evaluating nonradiative transition rates occurring in a multidimensional space. A suitable normalization criterion allows the attainment of simple formulas [Eqs. (11) and (12)] that yield, as a limiting case [Eq. (7)], the usual approximation of considering only one contribution, that corresponding to the least-action path.

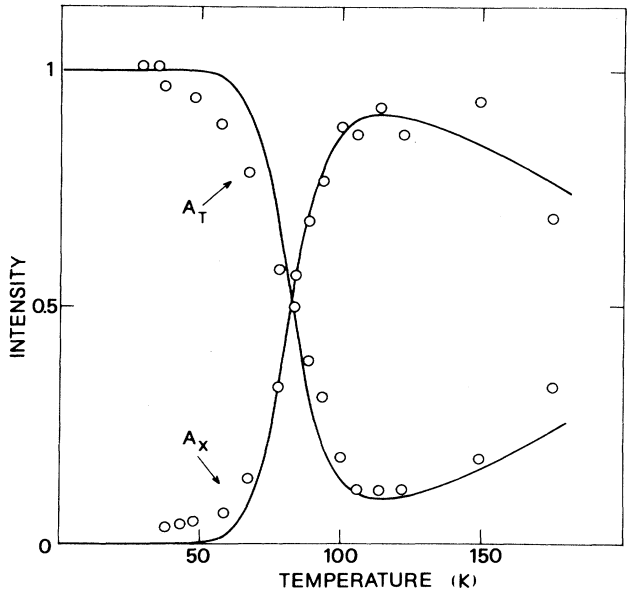

FIG. 8. Same as Fig. 7 for KBr:Tl. Solid lines: after Eqs. (21) with $E_T=653$ cm^{-1}, $E_X=1014$ cm^{-1}, $\Delta E=361$ cm^{-1}, $\tau\nu=10^5$, and $K=5.37$.

Dealing with nonradiative transitions in a solid, one should be referring to a multidimensional space of an extremely high number of dimensions comparable to the number of normal modes of the system. Actually, the potentials are regarded as depending only on a few coordinates, the so-called interaction-mode coordinates,[22] which can be considered to represent in some average sense the lattice coordinates belonging to the same irreducible representation. This procedure is not restrictive as it seems, especially when applied to rather well-localized centers, as with Tl^+-like impurities. Within the adiabatic approximation, where the potential surfaces are determined independently of the nuclear kinetic energy, the interaction coordinates formally correspond (apart from the dimensions of coordinates and coupling constants) to the normal coordinates of the quasimolecular cluster including the impurity and its nearest-neighbor ions.

The potential model here considered is that relative to the $^3T_{1u}$ state in O_h symmetry. It consists of a tetragonal T minimum coexisting with two rhombic X minima.[18] The potential map of the $^3T_{1u,z}$ state is given in the subspace of the (Q_2,Q_3) tetragonal coordinates (Fig. 2). The potentials of the $^3T_{1u,x}$ and $^3T_{1u,y}$ states are completely equivalent to that of $^3T_{1u,z}$ apart from a rotation of $\pm\frac{2}{3}\pi$ in the Q_2,Q_3 plane, so we can consider only the $^3T_{1u,z}$ state. Really, these three states are linked by the trigonal modes (Q_4,Q_5,Q_6) so that a complete description of the potential should take into account the trigonal coordinates too. In the analysis of the intensities, however, the trigonal modes may be neglected while they become essential when other experimental features are studied.[18]

Owing to the shape of the potential, the normalized transmission coefficient (NTC) has been integrated over ϕ by a three-saddle-point approximation. Two isolated maxima, in the NTC-vs-ϕ curves (see Fig. 4), correspond to two well-separated classical paths for reaching the X minima, one for each minimum. Accordingly, a factor of 2 enters the kinetic equations [Eqs. (13)], which govern the population of the initial well. This is equivalent to multiplying by the same factor the transmission coefficient relative to only one classical path. This procedure, which has been rigidly applied in Ref. 6, becomes increasingly less

acceptable as the two paths of minimum action tend to coalesce. When the NTC-vs-ϕ curve becomes a bell-shaped function centered at $\phi=0$, we must consider only one contribution; hence the factor 2 must become 1. Following the method of the present work, we obtain the correct results. When the maxima of the NTC are well pronounced, the total transmission coefficient is nearly equal to twice the value corresponding to one path of minimum action ($D/D_{\max}\simeq 2$). When the maxima tend to coalesce, the factor decreases and tends to the unity (see Fig. 5). On the basis of these results, the temperature dependence of the A_T and A_X emission intensities of KI:Tl is obtained [through Eqs. (18)] more accurately with respect to the results of a previous work.[6] In particular, in Ref. 6 the A_X circles could not be made to lie on a single curve, whereas they do so in the present interpretation (Fig. 7).

We must recall, however, that the present results (as well as those of Ref. 6) have been obtained neglecting anharmonic effects, that is, assuming a uniform distribution of levels inside the initial well [$\rho(E)=(\hbar\omega)^{-1}$ in Eq. (19)]. This fact was indeed qualitatively considered in Ref. 6 in order to explain the variation of the fitting parameter $\hbar\omega/\xi$ with increasing temperature. A detailed account of the anharmonic effects, already difficult in the scheme of Ref. 6 which essentially employs a one-dimensional model, becomes more difficult in the present framework, which implies several potential cross sections, one for each value of ϕ. Thus we limit ourselves to give only a descriptive account. By considering a typical potential cross section,[6] we can estimate that the level density varies between 1 [in units of $(\hbar\omega)^{-1}$, at the bottom of the initial well] to ~ 1.3 near the top of the barrier where the deviation from the harmonic shape is more accentuated [for higher-lying levels, $\rho(E)$ is expected to be again ~ 1]. Therefore, as sketched by dashed line in Fig. 5, we see that the product $\rho(E)D/D_{\max}$ may give an indication of the involved approximation. In the previous computation of Ref. 6, $D/D_{\max}$ was maintained constantly equal to 2. This certainly implies a stronger approximation with respect to the present analysis with $\rho=1$, but $D/D_{\max}$ variable.

We can therefore conclude that the present work, although still affected by approximations, gives a better explanation of the temperature behavior of the Tl^+-emission intensities. More important is the fact that the inclusion of neighboring-path contributions to the classical contribution may represent an improvement of the semiclassical approach to this kind of problem.

ACKNOWLEDGMENT

This work was performed under support of the National Council for Research (Italy) in the framework of a bilateral project.

[1]M. V. Berry and K. W. Mount, Rep. Prog. Phys. 35, 315 (1972).
[2]T. Banks, C. M. Bender, and T. T. Wu, Phys. Rev. D 8, 3346 (1973).
[3]V. Z. Polinger, Fiz. Tverd. Tela (Leningrad) 16, 2578 (1974) [Sov. Phys.—Solid State 16, 1676 (1975)].
[4]A. I. Voronin, S. P. Karkach, V. I. Osherov, and V. G. Ushakov, Zh. Eksp. Teor. Fiz. 71, 884 (1976) [Sov. Phys.—JETP 44, 465 (1976)].
[5]M. C. M. O'Brien, J. Phys. C 9, 2375 (1976).
[6]A. Ranfagni, G. Viliani, M. Cetica, and G. Molesini, Phys. Rev. B 16, 890 (1977).
[7]R. A. Marcus and M. E. Coltrin, J. Chem. Phys. 67, 2609 (1977).
[8]N. Fröman, Phys. Rev. A 17, 493 (1978).
[9]K. Möhring and U. Smilansky, J. Chem. Phys. 74, 4509 (1981).
[10]A. Ranfagni, D. Mugnai, and R. Englman, Phys. Rev. B 23, 4140 (1981).
[11]R. Englman and A. Ranfagni, Physica 98B + C, 151 (1980); 98, 161 (1980).
[12]R. P. Feynman and A. R. Hibbs, *Quantum Mechanics and Path-Integrals* (McGraw-Hill, New York, 1965).
[13]M. S. Marinov, Phys. Rep. 60, 1 (1980).
[14]J. P. Sethna, Phys. Rev. B 24, 698 (1981).
[15]A. Ranfagni, Phys. Lett. 62A, 395 (1977).
[16]D. Mugnai, A. Ranfagni, and R. Englman, Phys. Lett. 94A, 12 (1983).
[17]L. J. Schiff, *Quantum Mechanics* (McGraw-Hill, New York, 1955).
[18]D. Mugnai, A. Ranfagni, and G. Viliani, Phys. Rev. B 25, 4284 (1982), and references therein.
[19]L. B. Felsen and N. Marcuvitz, *Radiation and Scattering of Waves* (Prentice-Hall, Englewood Cliffs, N.J., 1973), Chap. 4.
[20]W. Magnus, F. Oberhettinger, and R. P. Soni, *Formulas and Theorems for the Special Functions of Mathematical Physics* (Springer, Berlin, 1966), Chap. 8.
[21]R. Illingworth, Phys. Rev. 136, A508 (1964).
[22]Y. Toyozawa and M. Inoue, J. Phys. Soc. Jpn. 21, 1663 (1966).